Anal Bioanal Chem (2016) 408:2697–2705
DOI 10.1007/s00216-015-9287-9

TRENDS

Nanoparticle chains as electrochemical sensors and electrodes

Long Pu[1] · **Maarij Baig**[1] · **Vivek Maheshwari**[1]

Received: 3 November 2015 / Revised: 14 December 2015 / Accepted: 18 December 2015 / Published online: 12 January 2016

Abstract With the advances in the field of nanotechnology, significant progress is being achieved in fabrication of nanoscale electrodes (nanoelectrodes) and using their properties for applications in multiple fields. Compared with conventional macroscale electrodes, nanoelectrodes offer many advantages that arise from their limited size. Self-assembled chains of metal nanoparticles in particular have drawn interest for fabrication of nanoelectrodes because of their unique electrical properties and geometric morphology. This article discusses the fabrication methods and potential applications of nanoparticle chains as nanoelectrodes in electrochemical systems and also as conductometric sensors. The challenges for such systems are also summarized.

Keywords Biosensors · Electroanalytical methods · Electrochemical sensors · Nanoparticles/nanotechnology

Published in the topical collection featuring *Young Investigators in Analytical and Bioanalytical Science* with guest editors S. Daunert, A. Baeumner, S. Deo, J. Ruiz Encinar, and L. Zhang.

Long Pu and Maarij Baig contributed equally to this work.

Electronic supplementary material The online version of this article (doi:10.1007/s00216-015-9287-9) contains supplementary material, which is available to authorized users.

✉ Vivek Maheshwari
vmaheshw@uwaterloo.ca

[1] Department of Chemistry, The Waterloo Institute of Nanotechnology, University of Waterloo, 200 University Ave. West, Waterloo, ON N2L 3G1, Canada

Introduction

With the rapid development in technology, there is a fast-growing market for a diverse range of electrochemical sensing applications, from portable and wearable sensors to continuous health monitoring devices that meet the requirements for today's information-rich society. The electrode size is of critical importance in sensing applications as it defines the response characteristics of the system [1]. It determines the signal-to-noise ratio in the system, the profile of the diffusion layer and its evolution with time, the ohmic drop in the system, and the sample volume required for sensing [1]. Nanoscale electrodes (nanoelectrodes), because of their limited size, can significantly improve performance on the basis of these factors. Hence, research efforts are devoted to making this transition from macroscale electrodes (marcoelectrodes) to nanoelectrodes in electrochemical applications [2–4]. One of the primary advantages of nanoelectrodes is that with nanoscale components they are small enough to be used in size-limiting electronics [5, 6]—for example, when one is electrochemically sensing biomolecules in body fluids such as tears and sweat, the small sample volume required in a nanoelectrode system is a significant advantage [4]. Nanoelectrodes are hence critical for applications in portable/wearable devices. Further, by incorporation of multiple nanomaterials in the nanoelectrodes, their properties can be made multifunctional, targeting more than one analyte. The advantages of the small size of the nanoelectrode compared to a macroelectrode also result from the small electrical double layer and multidimensional analyte diffusion layer formed on its surface [3, 4, 7, 8]. This leads to a rapid response and a short stabilization time, which notably improve the performance of a sensing system. It also translates to a higher charge/discharge rate for the nanoelectrode when it is used in energy storage systems [9, 10]. Because of these properties

and their nanoscale dimensions, sensing of biomolecules is one of the primary fields of application for nanoelectrodes. Modified nanoelectrodes have been developed for accurate and sensitive detection of a number of biomarkers and molecules, such as glucose, prostate-specific antigen, iodine, cytochrome *c*, blood cholesterol, urea, IgG, galactose, and lactic acid [11, 12]. Recently, dopaminergic neurons used in stem-cell therapy for Parkinson's disease were distinguished from other types of cells by use of a nanocup electrode array [12]. The reduced electrode dimensions also lead to a smaller ohmic drop and a higher signal-to-noise ratio in the system, hence generating reduced energy losses and heating in the system and a signal with higher fidelity, which is crucial for continuous-monitoring wearable devices [13, 14]. More detailed discussion on the characteristics of nanoelectrodes has been the subject of many recent reviews [3, 5, 14]; here we focus on the recent progress to assemble such electrodes with use of nanoparticles and their chains.

Given the properties of nanoelectrodes, intense research efforts are being devoted to their fabrication and application in multiple fields [3, 5, 7, 9, 13]. As a result, there has been a significant increase in the number of publications on this topic (Fig. 1a) since the early reports on the use of nanoelectrodes [15–17]. There is an increasing trend of using nanoparticle chains as a nanoelectrode [18–23]. We briefly discuss two kinds of nanoparticle chain electrodes, one made by self-assembly [24] and the other made by dielectrophoresis (DEP) [23]. The primary difference is that in one case the nanoparticles are first self-assembled into chains and then deposited as electrodes, whereas in the second case nanoparticles are deposited under dielectrophoretic forces and form chain-like structures under controlled conditions. Compared with a monolithic electrode of the same size, nanoparticle chains (and their arrays) have distinct electrical properties, such as characteristic coulomb blockade, nonlinear current–voltage characteristics, and sensitivity to gating and the local environment [25–27]. Being a chain-like structure, they also become electrically conducting below the percolation threshold for random arrays. The charge transport (or current flow) in these chains is the result of the charge carriers being subjected to a series of junctions as they traverse the constituting nanoparticles because of an applied bias [25]. This controllable and discreet transfer of electrons (charge carriers) between the small conducting "islands" (the nanoparticles) in these chains leads to their observed characteristic electrical properties. The highly sensitive characteristics (on the scale of a single electron) of these chains present an opportunity for applications in various devices [26, 28]. Yu et al. [18] have shown that Au nanoparticle chains can detect cellular activities as transistors while interfaced with live cells in aqueous medium. Our group has made multifunctional materials by electrochemical synthesis on Au nanoparticle chain electrodes

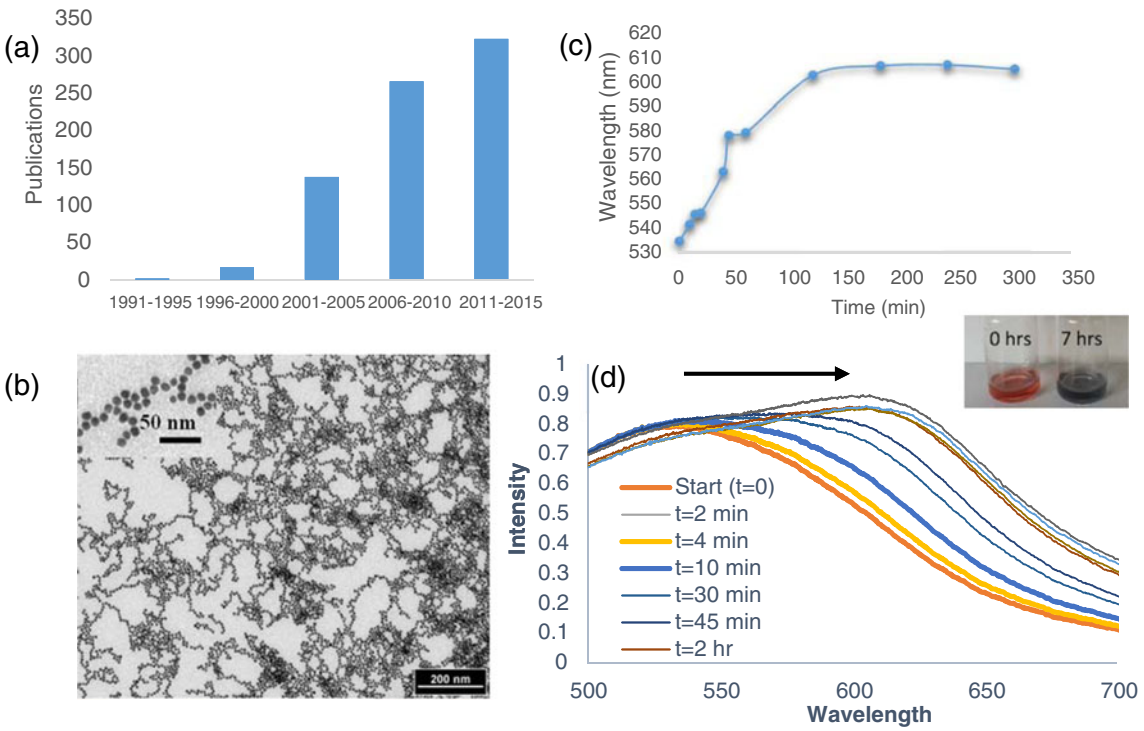

Fig. 1 **a** Increase in the number of publications on nanoelectrodes during the past 25 years. **b** The transmission electron microscopy image clearly shows the assembly of the nanoparticles into branched chain structures. The higher-magnification image in the *inset* shows that Au nanoparticles are separated by 1–2 nm. **c** Change in wavelength (at peak intensity) with time of the Au nanoparticle plasmon resonance due to self-assembly. **d** Ultraviolet–visible absorbance plot of the self-assembly progress of Au nanoparticles and Mn^{2+} ions. The *red line* is a scan of the Au nanoparticle solution in absence of Mn^{2+}. The *inset* shows the color change on self-assembly from the initial solution (*left to right*)

[22]. Mutual modulation between the chains and the synthesized nanomaterials was characterized by our group. This article focuses specifically on chains made with Au nanoparticles as they are widely used as an electrode material in electrochemical sensors and devices, because of their commercial availability, biocompatibility, well-characterized properties, and thermodynamically stability.

Self-assembled Au nanoparticle chain electrodes

Constructing nanoelectrodes with a single nanoparticle is a challenging task given the complexity of forming electrical contacts on such a scale and generating a measureable response with simple electronics [7, 29]. In contrast, a conductive pathway formed by chains of nanoparticles on the scale of micrometers is more facile to fabricate and configure as an electrode while maintaining the characteristics associated with a nanoelectrode [19, 21, 23]. Self-assembly can be an easy and cost-effective method to organize nanoparticles into chains. Typically, nanoparticles are stabilized with capping agents to form stable colloidal suspensions [30]. The functionality of the capping agent has been used to self-assemble these nanoparticles into distributed chains (branched 1-D arrays) [22, 24, 30]. Both the reported examples discussed below use citrate-capped Au nanoparticles and a controlled addition of multivalent cations to self-assemble them into distributed chains. These chains are then deposited on a substrate functionalized with (3-aminopropyl)triethoxysilane (or with NH_3 plasma) [19].

The citrate-capped Au nanoparticles suspended in aqueous medium have a negative zeta potential and are brought into close physical proximity through ionic linkers (e.g., Zn^{2+}, Ca^{2+}, Fe^{3+}). The nanoparticles and linkers self-assemble to form nanoparticle chains, as seen in a typical transmission electron microscopy image (Fig. 1b); here the nanoparticles are assembled with use of Ca^{2+}. If the concentration of the linker is too low, the assembly of chains is impeded because of insufficient interaction between adjacent nanoparticles. Increased concentration of the linker can cause the nanoparticles to aggregate and precipitate. The assembly progress is monitored by visual inspection and by ultraviolet–visible spectrophotometry as it indicates the assembly of the 0-D nanoparticle into higher ordered nanostructures. Figure 1c shows typical ultraviolet–visible spectrophotometry plots obtained from monitoring the assembly process using Mn^{2+} ions. The peak wavelength absorbance associated with the surface plasmon of the nanoparticles undergoes a redshift (Fig. 1d) because of its delocalization over adjacent nanoparticles on self-assembly. The use of these self-assembled nanoparticle chains as electrodes is discussed below on the basis of two reported examples.

Our group reported a device that was built by electrochemical synthesis on nanoelectrodes made with these self-assembled nanoparticle chains [22]. Divalent Ca^{2+} ions are added to the Au nanoparticles (10–12 nm) to form self-assembled micrometer long-chain networks of Au nanoparticles. These nanoparticle chains are then passively deposited on the insulating gap between two gold electrodes on a (3-aminopropyl)triethoxysilane-functionalized chip (see Fig. 2a). The deposited chains are electrically conducting and show typical effects such as a threshold voltage (V_T; below which there is no conduction) and oscillations in conductance (Fig. 2b) that are the manifestation of electron flow through a series of isolated nanoparticles. These chains were then used as nanoelectrodes for in situ electrochemical synthesis of nanomaterial (ZnO nanorods) directly on the nanoparticle chains. During the process the underlying nanoparticles serve as electrochemically active sites, because of the electrical conduction of these chains and the catalytic nature of the constituent Au nanoparticles. The second layer, ZnO nanorods, was successfully fabricated on their surface as a result. The nanoscale electrochemical process results in the formation of nanorods that are in direct contact with the nanoparticles and also spatially confined by them. The field emission scanning electron microscopy images (Fig. 2c) confirm that the Au nanoparticle chains are the specific location for the growth of the ZnO rods. The size of the ZnO nanorods matches well with the size of the Au nanoparticle chains, which confirms that Au nanoparticles act not only as conducting pathways in the electrochemical deposition but also as preferential growth sites for ZnO. The typical hexagonal shape of ZnO and the underlying bright Au chains can be seen in Fig. 2d. The resulting ZnO–Au hybrid system combines the individual characteristics of the Au nanoparticle array and the ZnO nanorod pathway. The direct interfacing also leads to mutual intermodulation between the two systems.

By observation of the effect of light intensity on the parameters V_T and α (which characterizes the dimensionality of the Au matrix), the influence of the ZnO nanorods on the Au chains was examined. For the hybrid device, $\alpha \sim 2.45$ was observed, which matches with the array being a 2-D matrix of nanoparticles with 1-D bottlenecks for conduction. No significant change in α was observed (Fig. 2e) on illumination of this hybrid with ultraviolet light, which would lead to photoexcitation of the ZnO nanorods. This is expected as the underlying dimensionality of the Au matrix is not affected by the generation of the electron–hole pairs in the ZnO rods. However, photoexcitation of ZnO nanorods changes the threshold voltage significantly. Figure 2e shows the decrease in V_T on illumination. The phenomenon is similar to gating on these arrays by an external electric field. Because ZnO is a semiconductor, electron–hole pairs are generated in ZnO under illumination, and the surface defects on the nanorods trap the holes, which locally gate the Au nanoparticles and alter the threshold voltage on Au nanoparticle chains. Further increase of the light intensity results in a stabilization of the threshold

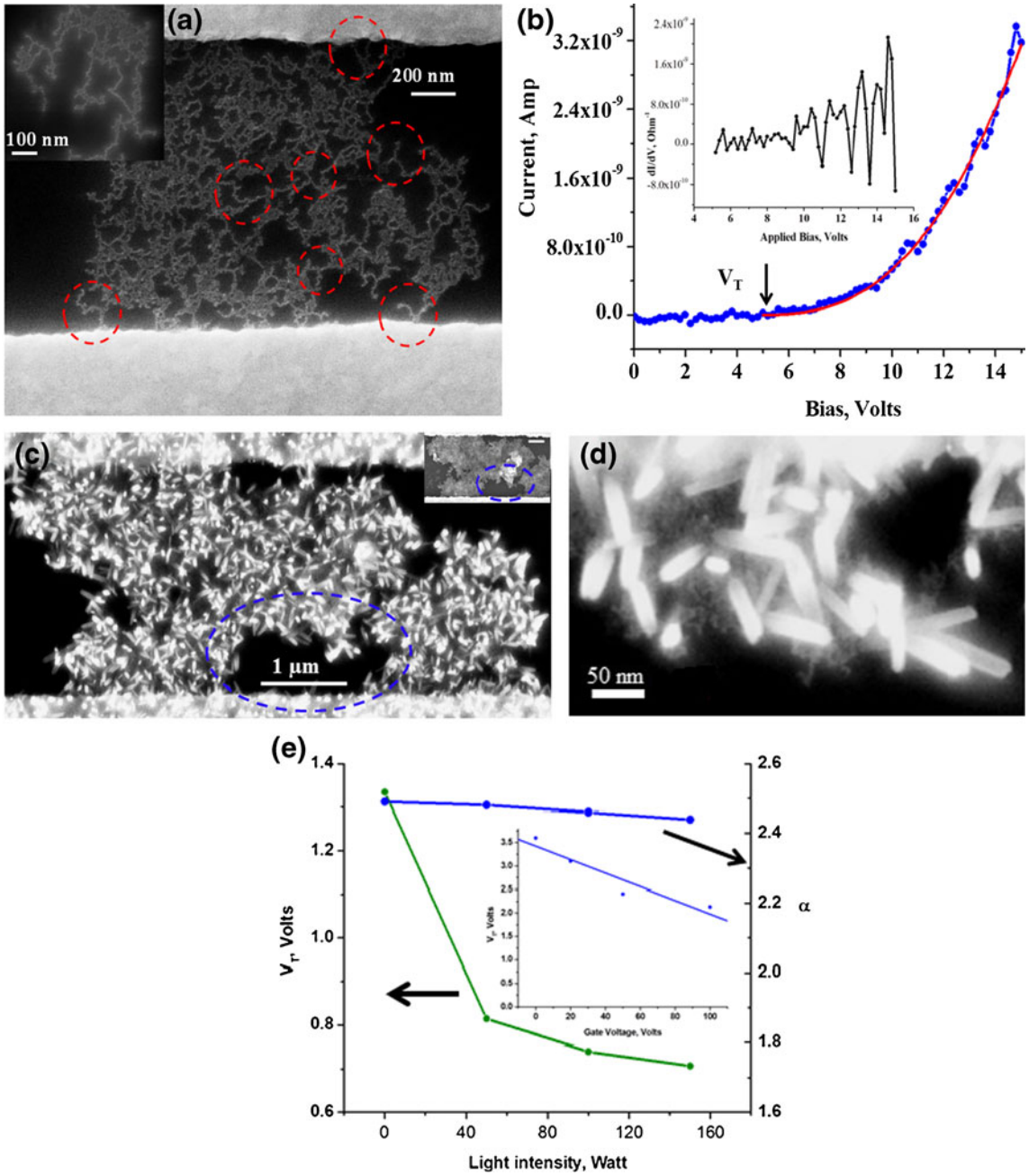

Fig. 2 **a** Au nanoparticle chains which are passively deposited bridge the gap between two Au pads and form a conductive pathway. Bottlenecks with 1-D chains are highlighted by *red circles*. **b** *I–V* response of Au nanoparticle arrays shows a threshold voltage V_T. The *inset* shows a plot of the differential conductance, and oscillations in it are observed. **c** ZnO nanorods are clearly observed on the nanoparticle chains. The *inset* shows the array before synthesis. **d** The ZnO nanorods have a size of approximately 20–30 nm and are growing directly from the nanoparticle chains. **e** Effect of light intensity on V_T and α. (From [22] with permission)

voltage; this can be explained by the saturation of electron–hole pairs at high light intensity. The photosensitivity of ZnO is able to modulate the characteristics of the underlying Au chains because of direct interfacing of the two nanomaterials.

The ability of these nanoparticle chains to function as an electrochemical electrode illustrates their potential for generating hybrid combinations of nanomaterials with multifunctionality. Because they assembled from 10–12-nm Au nanoparticles, their nanoscale structure leads to reactions that are locally confined on a similar scale, as illustrated by the diameter of the ZnO nanorods. This is an important characteristic that shows that these chains successfully function as nanoelectrodes.

Electrochemical characteristics of nanoelectrodes made by self-assembled nanoparticle chains, similar to the ones discussed above, were studied by Lee et al. [20]. By modulating the density of the passively deposited Au nanoparticle network, they fabricated ultramicroelectrodes (UMEs) as well

as nanoelectrode ensembles (NEEs). The density of deposition was controlled by variation of the deposition time from 6 to 24 h. The 24-h sample with a high density of the chains showed behavior indicative of a radial diffusion pattern such as a sinusoidal steady-state current. This UME-like behavior was further confirmed by the observation that the potential for the maxima of the reduction current (I_{red}) is independent of the scan rate (ν). In comparison, a planar macroelectrode shows a linear dependence, as seen in Fig. 3a. The maxima of the reduction current on the planar electrode show a typical

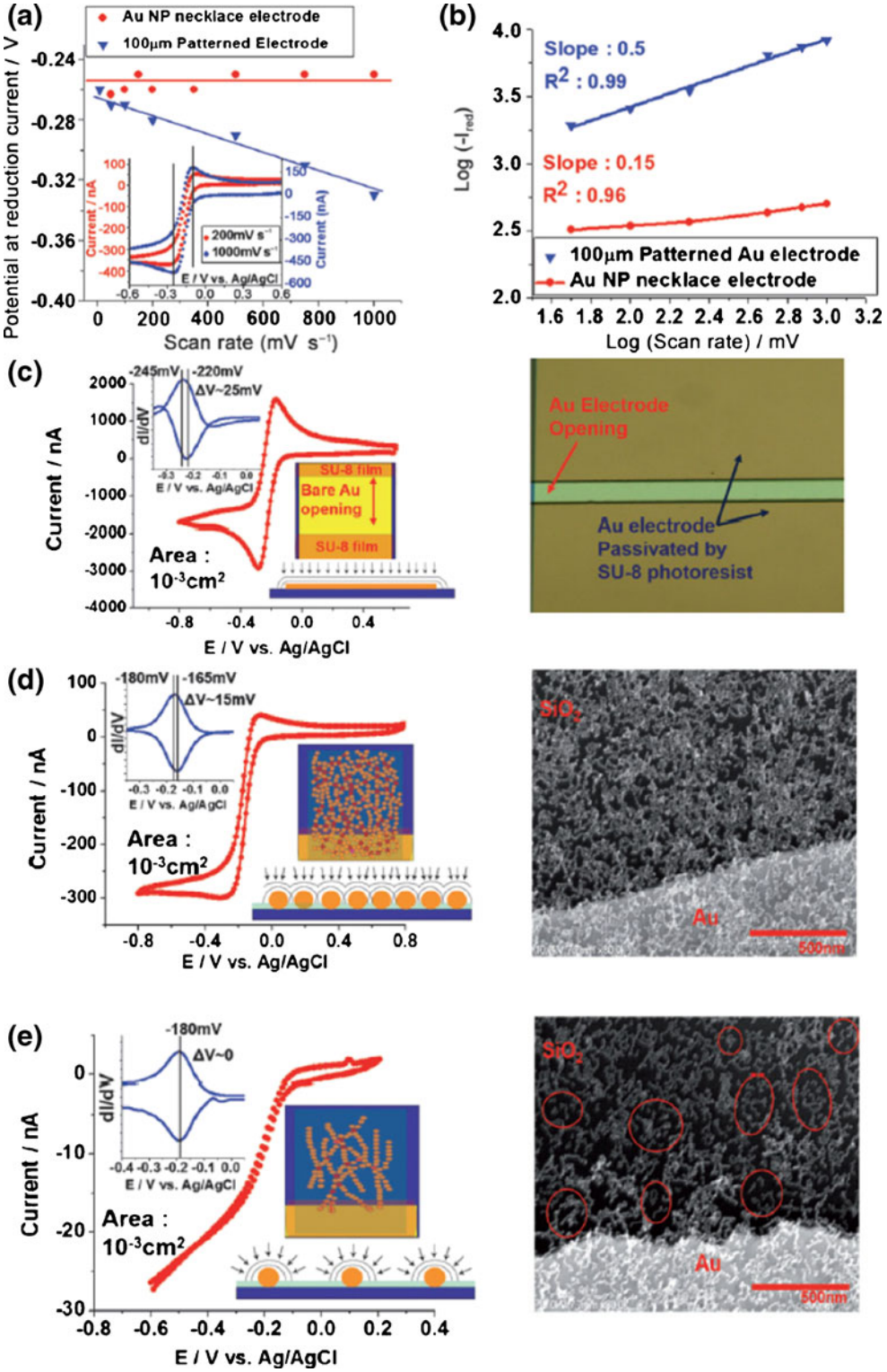

Fig. 3 **a** Change in potential at reduction current as a function of scan rate [100 μM $Ru(NH_3)_6^{3+}$ in 1 mM KCl]. The *inset* shows cyclic voltammograms at 200 and 1000 mV/s of nanoparticle arrays. **b** Scaling law for reduction current as a function of scan rate [100 μM $Ru(NH_3)_6^{3+}$ in 1 mM KCl]. **c**–**e** Comparison of electrodes: **c** a planar bare Au electrode, **d** a 24-h-deposited nanoelectrode, and **e** a 6-h-deposited nanoelectrode. From *left to right* in each plot, a cyclic voltammogram of 100 μM $Ru(NH_3)_6^{3+}$ at 200 mV/s, with the *left inset* showing the derivative of current and the *right inset* showing a schematic of the diffusion layer, and images of the electrode (*red circles* indicate some nanoparticle strands not connected to the network). *NP* nanoparticle. (From [20] with permission)

dependence on the scan rate, ν, as $I_{red} \approx \nu^{0.5}$, indicating a diffusion-controlled redox reaction. In contrast, the high-density nanoparticle chain electrode has a significantly smaller slope of 0.15 (Fig. 3b). This weak dependence indicates that there is limited overlap between the individual radial diffusion profiles of the nanoparticles constituting the electrode. A complete overlap would lead to a monolithic diffusion profile on the electrode and it would have characteristics similar to those of a macroelectrode. Some linear diffusion was indicated by the weak dependence.

To further enhance the characteristics and make a transition to NEEs, lower density of the chains was deposited by reduction of the deposition time from 24 to 6 h; as a result, the coverage was decreased from 54 to 26%. As the chains have a linear branched structure, they are still electrically conducting at 26% area coverage, which is below the percolation threshold of a random 2-D array. As the coverage is decreased, NEE behavior is observed, indicating that the electrode characteristics are dominated by radial diffusion. The difference in the half-wave potential (ΔV) of the forward and the backward scan of cyclic voltammetry decreases from approximately 25 mV for a planar Au electrode to approximately 15 mV for 54% Au chain coverage and to approximately 0 mV for 26% chain coverage (Fig. 3c–e, respectively). This behavior was further verified by electrochemical impedance spectroscopy results that characterize the charge transfer resistance and the electrical double layer capacitance.

The UME and NEE characteristics of the Au-chain-based electrode and the ability to control this transition based on the density of deposition as presented in this work shows that the chain-like structure leads to significant differences in comparison with just a 2-D array of nanoparticles. Their ability to function as UMEs and NEEs is attributed to this 1-D chain-like structure. The Au chains show the typical characteristics of the radial diffusion profile even though the nanoparticles are close to each other and are electrically conducting even below the percolation threshold of random 2-D arrays. The two examples presented above show that these chains can be a crucial building block for making nanoelectrodes and then can be used for development of sensors and devices based on their characteristic diffusional and electrical properties. They can also be used to develop hybrid nanoscale materials with multifunctional properties.

Nanoelectrodes based on dielectrophoresis techniques

Dielectrophoretic forces have also been used for deposition of Au nanoparticles as electrodes. Instead of passive deposition as discussed earlier, here an alternating electric field is applied

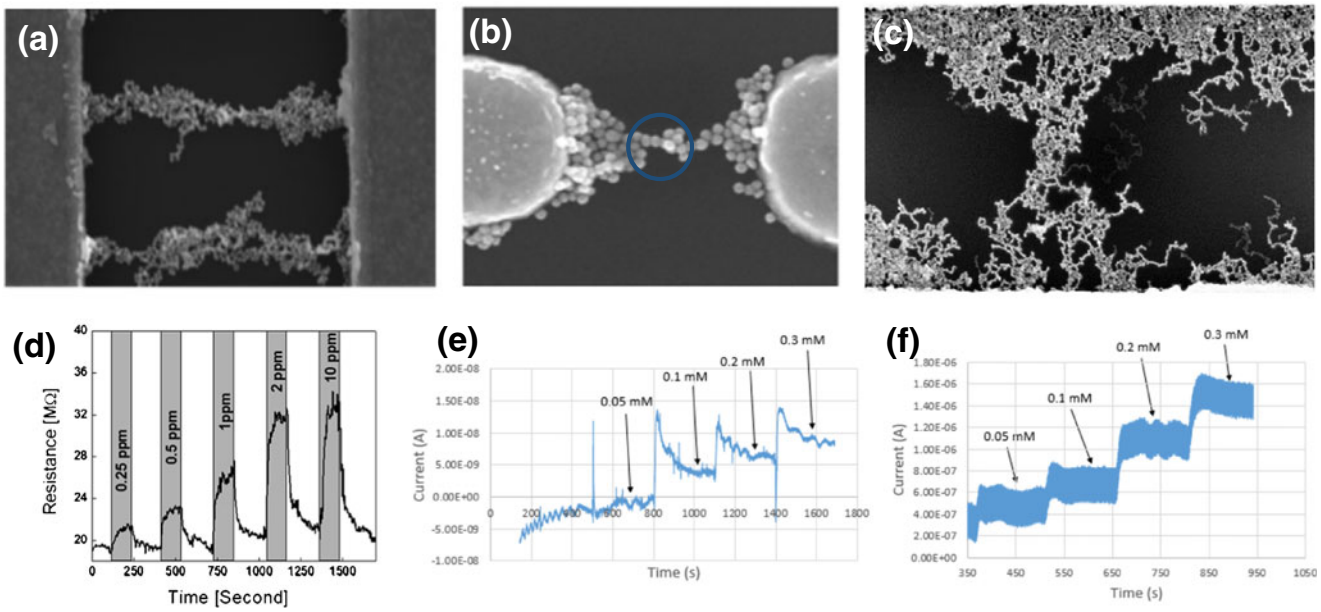

Fig. 4 Au nanoparticle chain nanoelectrodes fabricated by application of dielectrophoresis with use of **a** 38-nm glycine-capped Au nanoparticles, **b** 60-nm citrate-capped Au nanoparticles, and **c** 10-nm citrate-capped Au nanoparticles. Tight junctions can be observed (*blue circle*). **d** Increasing concentration of H_2S detected on the basis of resistance change of the Au nanoparticle chain nanoelectrode. *Dark bands* indicate H_2S exposure. *White bands* indicate dry air exposure for purging H_2S from the sensor surface. Steady-state current response of **e** nanoelectrode and **f** micrometer-scale electrode in stirred conditions in 1× phosphate-buffered saline (pH 7.4). Aliquots of glucose were added to increase the concentration in the range of 0.05–0.3 mM. (From [21, 23] with permission)

to induce dipoles (and higher poles) in the metal nanoparticles [31–33]. Simultaneously, a spatial gradient in the electric field leads to a force on the nanoparticles and causes their deposition. DEP is a well-known technique used for deposition of a variety of materials of varied composition, shape, and size. This technique has been well studied and discussed in many reviews [34, 35]. Typically, the deposition is conducted between two micrometer-scale electrodes separated by a micrometer-scale gap, immersed in an aqueous medium containing the Au nanoparticles. On application of the electric field, the nanoparticles deposit at the electrodes and with time lead to the bridging of the gap between them. The magnitude of the dielectrophoretic force can be controlled by the frequency and amplitude of the applied electric field. Combined with these controls and the time for which the dielectrophoretic force is applied, the density of the Au nanoparticle deposition can be modulated. Deposition can be performed with either a plain Au nanoparticle solution containing individual nanoparticles or a solution containing self-assembled Au chains. Typical examples of these depositions are shown in Fig. 4, where Fig. 4a and b shows the result of deposition with just a plain Au solution and Fig. 4c shows the result of a DEP-based deposition conducted in our group using the self-assembled chains. The DEP-based method confines the deposition of the nanoparticles to the region where the gradient in the electric field is generated, and this is usually between the two electrodes. The advantage of having control over the magnitude of the force and the region of its application is that both the spatial location of deposition and its density can be easily controlled.

The DEP-based deposition of the Au nanoparticle chains can be monitored in real time with an optical microscope. It can also be observed electrically by monitoring of the voltage drop across a resistor arranged in series with the electrodes and the gap between them, over which the dielectrophoretic force is applied [23]. As the Au nanoparticles deposit, the voltage drop across the resistor increases gradually. At the point where the depositing nanoparticles form an electrically conducting bridge between the two electrodes, the voltage drop across the resistor jumps. This occurs as there is now a flow of current between the two electrodes through the deposited Au nanoparticle bridge. The real-time electrical monitoring setup is advantageous for industry and academia looking to fabricate nanoelectrodes using the DEP method. Also it helps avoid prolonged exposure to the high voltage used for DEP after the contact between the micrometer-scale electrodes has been established by the depositing Au nanoparticles, as this can damage their nanostructure. Implementation of this method to observe in real time the formation of the Au nanoparticle bridge can be crucial for industry-scale automated fabrication of nanoelectrodes [23].

Following the formation of the Au nanoparticle bridge between the two micrometer-scale electrodes, the conduction mechanism across the Au nanoparticles can be used for sensing of organic compounds in liquids and gases. The electron conduction across the Au nanoparticles (when their deposition density is limited) as discussed above will have characteristic features such as coulomb blockade and will be based on sequential tunneling (or hopping) of electrons (or charge carriers) between adjacent nanoparticles [21]. The absorption of molecules on the Au nanoparticle surface causes a change in the tunneling barrier, modulating the electrical conduction across the Au bridge. This sensitivity in electrical conduction has been used for sensing organic compounds in gas and in liquid. For example, a nanoelectrode has been shown to selectively detect H_2S at room temperature [21]. Adsorption and desorption of H_2S molecules results in a drastic change in resistance of the gold nanoparticle chains (Fig. 4d).

Response time, recovery time, and detection limit were characterized. The sensor showed a sensitivity of 29.84% ppm^{-1}, a sub-parts per million detection limit, an upper detection limit of 2 ppm, and a response time of less than 20 s for 10 ppm H_2S [21]. Interfering gases such as CO, SO_2, and NH_3 were shown to produce a negligible change in signal. Maximum sensitivity was observed when the density of the Au nanoparticles was limited to avoid multilayer overlapping deposition and lead to a 1-D conduction regime. Although this sensing of analyte molecules is based purely on the change in the electrical resistance, it shows that Au nanoparticle assemblies can be used as electrodes and their deposition configuration is critical in determining their sensitivity.

DEP-based deposition was also applied by our group to the self-assembled chains discussed previously. A typical deposition results in the formation of a limited density bridge by the Au chains between the two micrometer-scale Au electrodes. Following this, similarly to the formation of ZnO nanorods, Pt was electrochemically synthesized on these chains. Pt serves as a catalyst for the detection of glucose molecules. The hybrid structure of the Au chain nanoelectrode and Pt was then characterized for its glucose sensing capability, and this was compared with that of a micrometer-scale electrode. The micrometer-scale electrode was made by electrodeposition of Pt on a micrometer-scale Au monolith. The response of the two electrodes for glucose sensing is shown in Fig. 4e and f. The absolute noise level in the system can be estimated by the vertical broadness of the current response as seen in Fig. 4e and f. The nanoelectrode has 500 times lower noise and 12,000 times greater sensitivity toward glucose than the micrometer-scale electrode. Micrometer-scale electrodes typically have higher current levels (microamperes to milliamperes) because of their higher electroactive surface area, but nanoelectrodes have a higher current density and consequently better signal-to-noise ratio and sensitivity. In the formation of nanoelectrodes using either Au chains or Au nanoparticles with either passive deposition or DEP, the density of the Au chains (and Au nanoparticles) has to be limited to prevent the

overlap of diffusion layers between adjacent nanoparticles. Each nanoparticle in the nanoelectrodes has an associated diffusion layer that grows in space with time and determines the mass transfer of the analyte molecules to its surface. This growing diffusional layer is a feature of the nanoelectrode that leads to its characteristic properties discussed above in comparison with macroelectrodes. If the nanoparticles are too close, their diffusion layers overlap and this leads to the formation of a monolithic diffusion layer. The nanoparticles then behave as a single entity and become similar to a macroelectrode in performance. Hence, control over the density of deposition is crucial to have nanoelectrode-like characteristics.

Outlook

The development of nanoparticle-chain-based nanoelectrodes will accelerate the advance of highly efficient wearable electronics. We presented in brief recent advances in the synthesis, characterization, and use of nanoelectrodes based on nanoparticle chains. Nanoelectrodes offer significant advantages over micrometer-scale electrodes—for example, significantly better signal-to-noise ratio, low diffusional resistance, and the requirement of very low sample volumes. In addition, these electrodes have a low ohmic drop and a rapidly growing 3-D diffusion layer, which results in rapid stabilization and response. Despite the low cost of fabrication, there are some challenges and opportunities associated with Au-nanoparticle-chain-based nanoelectrodes, which include (i) attaining high reproducibility in morphology and density, (2) selective deposition only at the target area, and (3) the opportunity for selective growth of functional material onto these nanoelectrodes. Generally, passive deposition methods use weak electrostatic forces to deposit nanoparticles on a surface. Their deposition time can range from minutes to hours, and the resulting structures have disordered morphology and non-uniform spatial density. The area of passive deposition can be controlled by use of low-resolution lithographic techniques [20]. Unlike passive deposition, DEP-based techniques can actively control AC field parameters to achieve reproducible morphology and density. In addition, base electrodes of a certain shape can be used to focus the electric field and control the deposition sites (see Fig. S1) [18]. Further, real-time deposition of the nanoparticles can be observed by monitoring of the voltage drop in the circuit [23]. This reported method needs to be further tuned to increase its sensitivity such that formation of limited density bridges with the Au nanoparticles can be observed and reproducibility in these nanoelectrodes can be achieved.

Despite the challenges, we believe nanoparticle chains will be a key constituent for building nanoscale electrochemical electrodes. Nanoparticle chains are anticipated to be a favorable route for synthesizing small electrodes because of their ability to preserve the nanoscale features and at the same time have a micrometer-scale size that makes their assembly into a cost-effective functional device easy. Further, by incorporation of secondary nanomaterials (such as ZnO and Pt), these Au chain nanoelectrodes can be tuned for multifunctionality and sensing of specific molecules. Another advance will be to interface the Au nanoparticles with enzymes specific to biomolecules of interest. As Au nanoparticles are widely used for anchoring of enzymes, this nanoelectrode–enzyme assembly will integrate biospecificity of enzymes with the advantages of a nanoelectrode. Self-assembled nanoparticle chains and photolithography, each with their own advantages and disadvantages, are complementary methods for fabricating nanoelectrodes. We believe the development of the next generation of nanoelectrodes will take advantages from both techniques to apply their characteristic properties for further advancement of the performance of current devices and sensors and also the development of new applications in multiple areas, such as biosensors, energy storage, and diverse catalytic systems.

Acknowledgments This work was supported by the University of Waterloo, the Canada Foundation for Innovation, Ontario Research Fund, and the Natural Sciences and Engineering Research Council of Canada.

Compliance with ethical standard

Conflict of interest The authors declare that they have no conflict of interest.

References

1. Bard AJ, Faulkner LR. Electrochemical methods: fundamentals and applications. 2nd ed. Hoboken: Wiley; 2001.
2. Freeman NJ, Sultana R, Reza N, Woodvine H, Terry JG, Walton AJ, et al. Comparison of the performance of an array of nanoband electrodes with a macro electrode with similar overall area. Phys Chem Chem Phys. 2013;15:8112–8.
3. Oja SM, Wood M, Zhang B. Nanoscale electrochemistry. Anal Chem. 2013;85:473–86.
4. Sun P, Mirkin MV. Kinetics of electron-transfer reactions at nanoelectrodes. Anal Chem. 2006;78:6526–34.
5. Cox JT, Zhang B, Penner RM. Nanoelectrodes: recent advances and new directions. Annu Rev Anal Chem. 2012;5(1):253–72.
6. Arrigan DWM. Nanoelectrodes, nanoelectrode arrays and their applications. Analyst (Cambridge, U K). 2004;129:1157–65.
7. Murray RW. Nanoelectrochemistry: metal nanoparticles, nanoelectrodes, and nanopores. Chem Rev. 2008;108:2688–720.
8. Godino N, Borrise X, Muñoz FX, Del Campo FJ, Compton RG. Mass transport to nanoelectrode arrays and limitations of the diffusion domain approach: theory and experiment. J Phys Chem C. 2009;113:11119–25.
9. Aricò AS, Bruce P, Scrosati B, Tarascon J-M-M, Schalkwijk WV. Nanostructured materials for advanced energy conversion and storage devices. Nat Mater. 2005;4:366–77.

10. Guo YG, Hu JS, Wan LJ. Nanostructured materials for electrochemical energy conversion and storage devices. Adv Mater. 2008;20:2878–87.
11. Yeh JI, Shi H. Nanoelectrodes for biological measurements. WIREs Nanomed Nanobiotechnol. 2010;2(2):176–88.
12. Kim TH, Yea CH, Chueng STD, Yin PTT, Conley B, Dardir K, et al. Large-scale nanoelectrode arrays to monitor the dopaminergic differentiation of human neural stem cells. Adv Mater. 2015;27(41):6356–62.
13. Compton RG, Wildgoose GG, Rees NV, Streeter I, Baron R. Design, fabrication, characterisation and application of nanoelectrode arrays. Chem Phys Lett. 2008;459:1–17.
14. Dawson K, O'Riordan A. Electroanalysis at the nanoscale. Annu Rev Anal Chem. 2014;7:163–81.
15. Menon VP, Martin CR. Fabrication and evaluation of nanoelectrode ensembles. Anal Chem. 1995;67(13):1920–8.
16. Baker WS, Crooks RM. Independent geometrical and electrochemical characterization of arrays of nanometer-scale electrodes. J Phys Chem B. 1998;102(49):10041–6.
17. Hulteen JC, Menon VP, Martin CR. Template preparation of nanoelectrode ensembles. Achieving the 'pure-radial' electrochemical-response limiting case. J Chem Soc, Faraday Trans. 1996;92(20):4029–32.
18. Yu C, Lee S-W, Ong J, Moore D, Saraf RF. Single electron transistor in aqueous media. Adv Mater. 2013;25:3079–84.
19. Lee EH, Lee SW, Saraf RF. Noninvasive measurement of membrane potential modulation in microorganisms: photosynthesis in green algae. ACS Nano. 2014;8:780–6.
20. Lee SW, Lee EH, Saraf RF. Dense array of nanoparticles as a large-area nanoelectrode for sensors: an oxymoron mesomaterial? ChemElectroChem. 2014;1(8):1281–6.
21. Lee J, Mubeen S, Hangarter CM, Mulchandani A, Chen W, Myung NV. Selective and rapid room temperature detection of H_2S using gold nanoparticle chain arrays. Electroanalysis. 2011;23(11):2623–8.
22. Pu L, Abbas AS, Maheshwari V. Electrochemical synthesis on nanoparticle chains to couple semiconducting rods: coulomb blockade modulation using photoexcitation. Adv Mater. 2014;26:6491–6.
23. Leiterer C, Berg S, Eskelinen A-P, Csaki A, Urban M, Törmä P, et al. Assembling gold nanoparticle chains using an AC electrical field: electrical detection of organic thiols. Sens Actuators, B. 2013;176:368–73.
24. Maheshwari V, Fomenko DE, Singh G, Saraf RF. Ion mediated monolayer deposition of gold nanoparticles on microorganisms: discrimination by age. Langmuir. 2010;26:371–7.
25. Likharev KK. Single-electron devices and their applications. Proc IEEE. 1999;87:606–32.
26. Parthasarathy R, Lin X-M, Elteto K, Rosenbaum TF, Jaeger HM. Percolating through networks of random thresholds: finite temperature electron tunneling in metal nanocrystal arrays. Phys Rev Lett. 2004;92:076801.
27. Suvakov M, Tadić B. Modeling collective charge transport in nanoparticle assemblies. J Phys: Condens Matter. 2010;22:163201.
28. Parthasarathy R, Lin X-M, Jaeger HM. Electronic transport in metal nanocrystal arrays: The effect of structural disorder on scaling behavior. Phys Rev Lett. 2001;87(18):186807.
29. Li Y, Cox JT, Zhang B. Electrochemical responses and electrocatalysis at single Au nanoparticles. J Am Chem Soc. 2010;132:3047–54.
30. Daniel M-C, Astruc D. Gold nanoparticles: assembly, supramolecular chemistry, quantum-size-related properties, and applications toward biology, catalysis, and nanotechnology. Chem Rev. 2004;104:293–346.
31. Hermanson KD, Lumsdon SO, Williams JP, Kaler EW, Velev OD. Dielectrophoretic assembly of electrically functional microwires from nanoparticle suspensions. Science. 2001;294:1082–6.
32. Bhatt KH, Velev OD. Control and modeling of the dielectrophoretic assembly of on-chip nanoparticle wires. Langmuir. 2004;20:467–76.
33. Kretschmer RWF. Pearl chain formation of nanoparticles in microelectrode gaps by dielectrophoresis. Langmuir. 2004;20:11797–801.
34. Barsotti RJ, Vahey MD, Wartena R, Chiang YM, Voldman J, Stellacci F. Assembly of metal nanoparticles into nanogaps. Small. 2007;3:488–99.
35. Xiong X, Busnaina A, Selvarasah S, Somu S, Wei M, Mead J, et al. Directed assembly of gold nanoparticle nanowires and networks for nanodevices. Appl Phys Lett. 2007;91:1–4.